Metabolic tagging reveals surface-associated lipoproteins in mycobacteria

Lia A. Parkin[1], Julian P. Maceren[2], Aseem Palande[3], Mary L. Previti[3], Jessica C. Seeliger[3,*]

Departments of [1]Microbiology and Immunology, [2]Chemistry, and [3]Pharmacological Sciences

Stony Brook University, Stony Brook, NY 11794, U.S.A.

* Contact: jessica.seeliger@stonybrook.edu

Keywords: lipoproteins, mycobacteria, surface proteins, fatty acids

ABSTRACT

Mycobacteria such as the causative agent of tuberculosis, *Mycobacterium tuberculosis*, encode over 100 bioinformatically predicted lipoproteins. Despite the importance of these post-translationally modified proteins for mycobacterial survival, many remain experimentally unconfirmed. Here we characterized metabolic incorporation of diverse fatty acid analogues as a facile method of adding chemical groups that enable downstream applications such as detection, crosslinking and enrichment, of not only lipid-modified proteins, but also their protein interactors. Having shown that incorporation is an active process dependent on the lipoprotein biosynthesis pathway, we discovered that lipid-modified proteins are also located at the mycobacterial cell surface. These data counter the commonly held assumption that mycobacteria do not move lipoproteins across the cell envelope and thus have implications for uncovering a novel transport pathway and the roles of lipoproteins at the interface with the host environment. Our findings and the tools we developed will enable the further study of pathways related to lipoprotein function and metabolism in mycobacteria and other bacteria in which lipoproteins remain poorly understood.

INTRODUCTION

Cell membranes are essential boundaries that maintain life. Accordingly, the inhibition of cell envelope biogenesis is a common mode of action among anti-bacterial drugs. Antibiotics against the human pathogen *Mycobacterium tuberculosis* (*Mtb*) are no exception, except that many target mycobacteria-specific pathways. In general, the mycobacterial cell envelope presents both opportunities and challenges in the fight against *Mtb*. On the one hand, pathways unique to mycobacteria offer prospects for selective inhibition; on the other hand, the mycobacterial cell envelope severely limits the permeation of diverse small molecules into the cytosol, including otherwise potent enzyme inhibitors, thus limiting cellular efficacy[1,2].

A strategy that incorporates both considerations is targeting processes in the cell wall whose inhibition not only compromises bacterial survival, but also sensitizes mycobacteria to other antibiotics. However, exploration of this approach is constrained by our limited understanding of cell wall biogenesis and cell wall processes overall. Even our basic knowledge of what proteins reside in the cell wall is limited by our incomplete understanding of export signals and by technical obstacles in accurately identifying cell wall proteins, although we and others have developed methods that are helping to build a better picture of this subcellular proteome[3–5]. In contrast to these unknowns, lipid-modified proteins known as lipoproteins are well established cell wall residents and the machinery that adds the post-translational modification is essential for *Mtb* survival[6–9]. In general, a conserved lipobox motif directs encoding proteins to the processing machinery[10,11]; while the lipobox is derived from studies in other bacteria, it is also found in mycobacteria. Based on this motif, lipoproteins make up ~3% of the total *Mtb* proteome (>100 lipoproteins, as predicted in several reports[10,11], including a recent review on mycobacterial lipoproteins[12]), consistent with the proportion predicted in other bacteria (1-3%)[13]. In our recent report of proteins identified by cell wall-specific protein tagging[3], proteins encoding a lipobox motif constituted 19% of the detected cell wall proteome (49 of 254 proteins). Otherwise, only a handful of individual mycobacterial lipoproteins have been experimentally confirmed[12].

Mtb lipoproteins are processed by a largely canonical pathway, based on bioinformatics and experimental validation in *Mtb* and other mycobacteria. In the consensus pathway, proteins with a lipobox motif are exported across the plasma membrane and into the cell wall via primarily the Sec secretion system, although a minority may traverse the Tat system[14]. Integral membrane proteins further process the nascent lipoprotein in the periplasm (**Figure 1**). First, lipoprotein diacylglyceryl transferase (Lgt; Rv1614)[15] catalyzes a thioether bond between diacylglycerol and the sidechain of a conserved cysteine (Cys) within the lipobox motif. Lipoprotein signal peptidase (LspA; Rv1539)[16] cleaves upstream of the modified Cys. Apolipoprotein N-acyltransferase (Lnt; Rv2051c)[17] then acylates the free amine of the now N-terminal Cys, yielding the mature, triacylated lipoprotein. All three enzymes are essential for *Mtb* survival[6–9]. While the LspA inhibitor globomycin inhibits *Mtb* growth, this activity appeared to be independent of LspA inhibition[18].
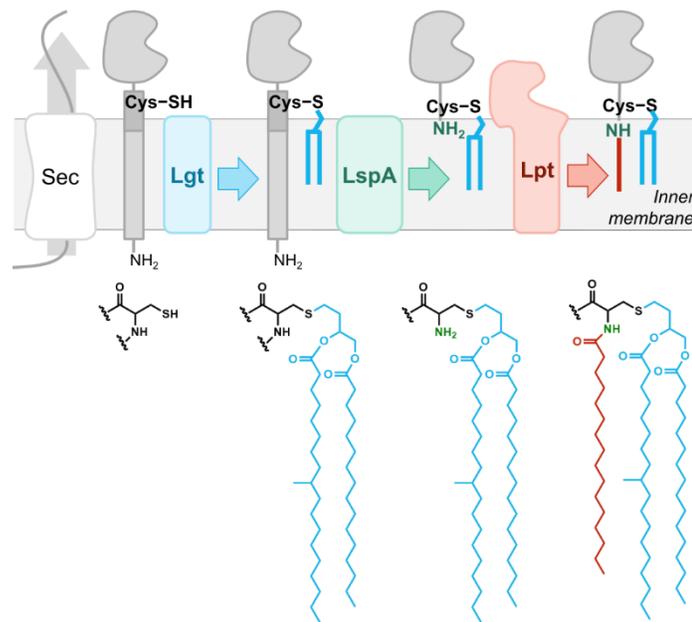
Figure 1. Fatty acids are incorporated into cell wall proteins via the lipoprotein processing pathway. Following export, primarily by the Sec secretion system, proteins are targeted for lipoprotein processing via a lipobox motif (dark grey fill) containing a conserved cysteine (Cys-SH). In the first committed step, Lgt modifies the Cys sidechain with a diacylglyceryl group via a thioether linkage (blue). LspA then cleaves the signal peptide, leaving the Cys as the N-terminal residue (green). Lpt then esterifies the amino terminus with a fatty acid (red), yielding the final N-terminally triacylated protein product. Fatty acid chains (16:0; 19:0) as reported[19]; one of two possible configurations for sn-1/sn-2 is shown and tuberculostearic acid is depicted as the most likely assignment for 19:0.

Interestingly, although the final enzyme Lnt is present in mycobacteria, diacylated forms are still detected, raising the question of whether these intermediates are functionally distinct from the mature, triacylated forms[17,19]. Also, mycobacterial Lnt activity lies within a bifunctional enzyme with two domains; the other domain is a polyprenol-monophosphomannose synthase involved in the synthesis of the mycobacterial lipoglycans lipomannan and lipoarabinomannan[20]. The possible connection between lipoprotein modification and lipid synthesis remains unexplored. Finally, while other diderm bacteria such as *E. coli* transport the majority of their lipoproteins to the outer membrane using the Lol pathway[21], mycobacteria lack direct Lol homologues, consistent with their closer phylogenetic relationship to monoderm gram positives[22]. Mycobacterial lipoproteins are thus assumed to reside exclusively in the plasma membrane, but the possibility that they transit to the mycobacterial outer membrane (also known as the mycomembrane) remains untested.

Lipoproteins have diverse functions in the cell wall, such as metabolite transport and cell wall synthesis; they have also been associated with virulence and host defense[12]. Of the 116 proteins most recently catalogued as lipoproteins, 78 have functional annotations, although many of these are only predictive[12]. Regarding the need for lipid modification, one hypothesis is that it serves as localization signal that facilitates function, for example, by positioning proteins proximal to membranes. Despite the diverse and critical roles lipoproteins play in *Mtb*, they remain poorly characterized with respect to their lipid modifications, with few experimentally verified exceptions. Overall, many mysteries remain regarding lipoprotein function and metabolism.

Experimental validation and characterization of lipoproteins has relied on metabolic labeling, mass spectrometric analysis, or a combination of bioinformatics and subcellular fractionation. A lipobox motif and detection in the membrane fraction[23–26] provide indirect evidence for individual lipoproteins. We recently reported experimental validation of 49 lipoproteins by compartment-specific proximity labeling using the engineered peroxidase APEX2[3]. Post-translational modification of the mycobacterial lipoproteins LpqH, LpqL, LprF, and LppX has also been characterized by mass spectrometry[19,27]. Incorporation of ^{3}H- or ^{14}C-fatty acids affords more direct evidence for the addition

of the lipid modification, as has been applied to LpqH[28] and LppX[29], but is not broadly accessible due to expense and safety and handling requirements for radioisotopes. Finally, none of these methods enable further downstream applications such as enrichment and identification.

We posited that fatty acid analogues that are tolerated by the lipoprotein synthesis machinery and enable other modes of detection would facilitate detailed study of individual lipoproteins and the lipoprotein proteome as a whole. Several modified fatty acids have been used to track fatty acid uptake and metabolism in mycobacteria, including in the context of infection, most notably those modified by the fluorophore BODIPY. THP-1-derived macrophage-like cells metabolize BODIPY C12 (BC12) into triacylglycerides (TAGs), which are then taken up by intracellular *Mtb*[30]. The related BODIPY FL C16 behaves similarly[31] and has been developed into an assay to quantify incorporation of host-derived BODIPY FL C16 (BC16) into intracellular *Mtb* by flow cytometry[32]. Mycobacteria in ex vivo infection and in vitro culture incorporate BC12, BC16m and/or their metabolites into intracellular lipid inclusions (ILI)[20,21,23]. Also, uptake of BC16 is dependent on proteins that stabilize the Mce1 and Mce4 transporter systems[31]. While these data support incorporation of fatty acid analogues into lipids, one study showed that *M. smegmatis* (*Msm*), a fast-growing non-pathogenic relative of *Mtb*, incorporated an alkynyl fatty acid into proteins[33]. The related species *Corynebacterium glutamicum*, which shares overall cell envelope architecture with mycobacteria, incorporated a similar medium-chain alkynyl fatty acid into mycolates on proteins, revealing a novel post-translational modification[34]; there have not yet been reports of mycoloylated proteins in mycobacteria such as *Msm*. Overall, fatty acid analogues show promise as labels for tracking lipid-modified metabolites, but their fates in mycobacteria have not been characterized.

In this work we explored the potential of BC12 and other fatty acid analogues to label proteins in mycobacteria. We found that BC12 readily labels proteins in both *Msm* and *Mtb* and thus provides a facile alternative to radiolabeling. We further showed that fatty acids containing functional groups compatible with click chemistry modification were also incorporated into proteins and enabled additional modes of detection, with the potential for downstream enrichment and identification.

Labeling was dependent on an enzyme in the lipoprotein biosynthesis pathway and was labile to base hydrolysis, supporting that modified proteins are lipoproteins. Using methods that selectively reveal surface-associated proteins, we found evidence that lipid-modified proteins are exposed at the cell surface, suggesting the transport of lipoproteins beyond the plasma membrane in mycobacteria. Overall, we validated a toolbox of readily available probes for tracking lipid-modified proteins that are expected to accelerate research into mycobacterial lipoprotein identification, synthesis, localization, and, most notably, transport.

RESULTS AND DISCUSSION

Mycobacteria metabolically incorporate a variety of fatty acid analogues into proteins

We first confirmed that the fluorescent fatty acid analogue BODIPY-C12 (BC12) is directly metabolized by mycobacteria. Based on previous studies, we hypothesized that BC12 would be incorporated by mycobacteria into lipids such as TAGs. Indeed, we found that *M. smegmatis* (*Msm*), a fast-growing, non-pathogenetic relative of *M. tuberculosis*, rapidly generated apolar lipids as the dominant fluorescent species, based on thin-layer chromatography analysis of solvent extracts and comparison to a standard generated by feeding BC12 to THP-1-derived macrophage-like cells (**Figure S1**).

Rangan et al. previously showed that another fatty acid analogue, alkynyl-fatty acid (alkFA; specifically, chain-length variant alk-14) labels proteins in multiple bacterial species, including *Msm*[33]. We correspondingly confirmed and further characterized protein modification by BC12. Fluorescence associated with proteins was BC12 dose-dependent and incorporation was abrogated in heat-killed cells, showing that incorporation is an active process (**Figure 2A**). Both *Msm* and *Mtb* incorporated BC12 into proteins and this signal was suppressed by the addition of OADC, a common growth medium supplement that includes albumin (0.5% w/v final concentration) and oleic acid (177 μM compared to 5 μM BC12) (**Figure 2A, B**). Addition of ADC, which contains albumin but not oleic acid,

similarly suppressed signal in *Msm*, indicating that sequestration by binding to albumin is a major factor in blocking BC12 incorporation into proteins (**Figure S2**).
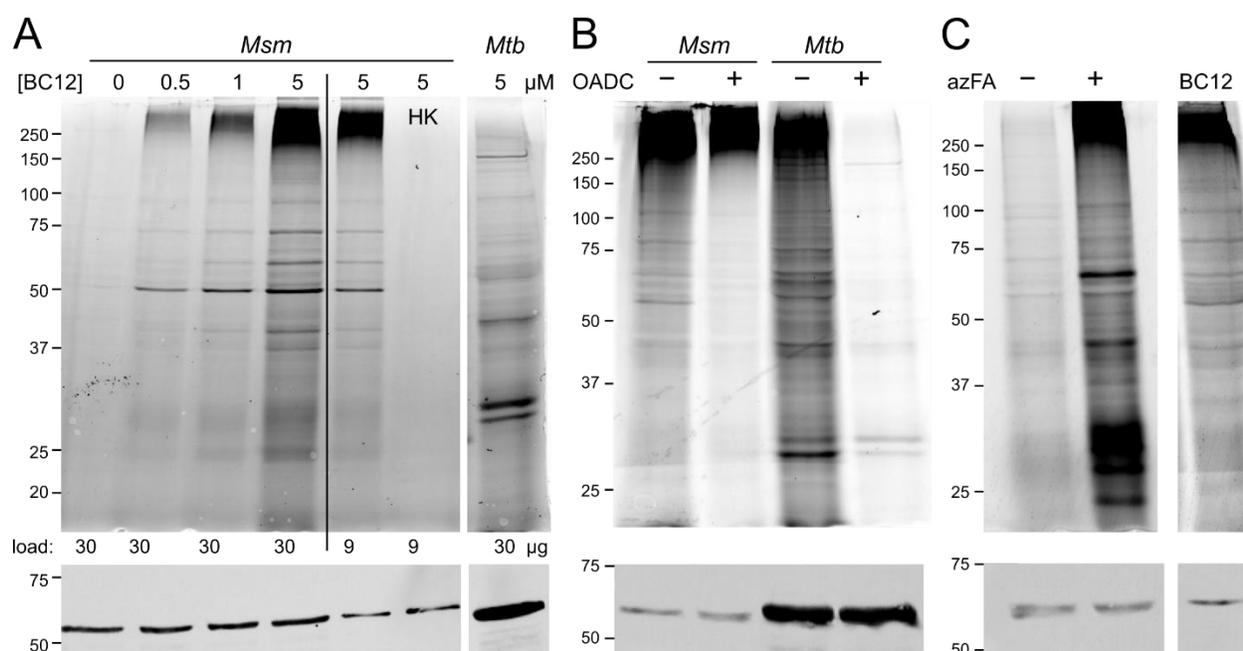
Figure 2. *Msm* and *Mtb* incorporate fatty acid analogues into proteins. A) *Msm* or *Mtb* was incubated with varying concentrations of BODIPY-C12 (BC12) for ~1 doubling time (2 h for *Msm*, 20 h for *Mtb*). Five µM BC12 was used for all subsequent experiments. Heat-killed (HK) cells served as a negative control and total lysates were analyzed by SDS-PAGE. B) Same as in A) except −/+ 10% OADC supplement during BC12 incubation. C) *Msm* was incubated with 20 µM azide-palmitic acid (azFA) or 5 µM BC12. All samples in each panel were run on the same gel; lanes scanned in separate detection channels appear slightly separated. Data are representative of at least n = 3 independent experiments.

We further tested the dependence of labeling on uptake using *Msm* Δ*mceG*[35], which lacks a factor required for the Mce import systems, most notably the fatty acid importer Mce1[31,36–38]. Protein labeling by BC12 trended towards being weakly dependent on *mceG*, with ~20% less fluorescence associated with proteins in the knockout vs. the complement strain (**Figure S3**). This mild reduction is not unexpected given that loss of *mceG* reduces ^{14}C-palmitate uptake by only ~50% in *Msm*[37]. Both observations suggest that other factors also determine fatty acid uptake, at least under these conditions; modified labeling conditions or kinetic measurements may reveal a more significant dependence on *mceG*.

Overall, our data supported BC12 feeding as a facile, accessible method to detect lipid modifications on proteins. Since a further goal is the experimental identification and validation of the

mycobacterial lipoproteome, we extended this method to other fatty acid analogues that would enable expanded opportunities for detection and affinity enrichment. We tested fatty acids modified with biotin or with functional groups that allow biorthogonal "click" coupling to a wide range of commercially available reagents. Incubating *Msm* with 12:0 N-biotinyl fatty acid (biotin-FA) did not yield any biotin-FA-dependent protein biotinylation (**Figure S4**). We speculate that the biotin moiety may be metabolized on the timescale of incubation (2 h), preventing detectable incorporation of the modified fatty acid into proteins. In contrast, and similar to an earlier report with alkFA[24], azido palmitic acid (azFA) was readily incorporated into *Msm* proteins, as detected after subjecting total lysates to copper-dependent azide-alkyne coupling (CuAAC) to a fluorescent alkyne (alk-Az488) (**Figure 2C**). In contrast, treatment of lysates with dibenzocyclooctyne (DBCO) reagents (DBCO-PEG4-biotin, DBCO-AF488) for strain-promoted azide-alkyne coupling (SPAAC) led to abundant signal that was not dependent on azFA (**Figure S2B,C**). This is likely due to azide-independent coupling to free thiols on cysteines[39]. Incubation with alkFA yielded protein labeling analogous to that obtained using azFA and also as previously reported[33] (**Figure 3A**). Overall, these results support CuAAC modification of incorporated azFA and alkFA as the most versatile approach for tagging lipid-modified proteins.
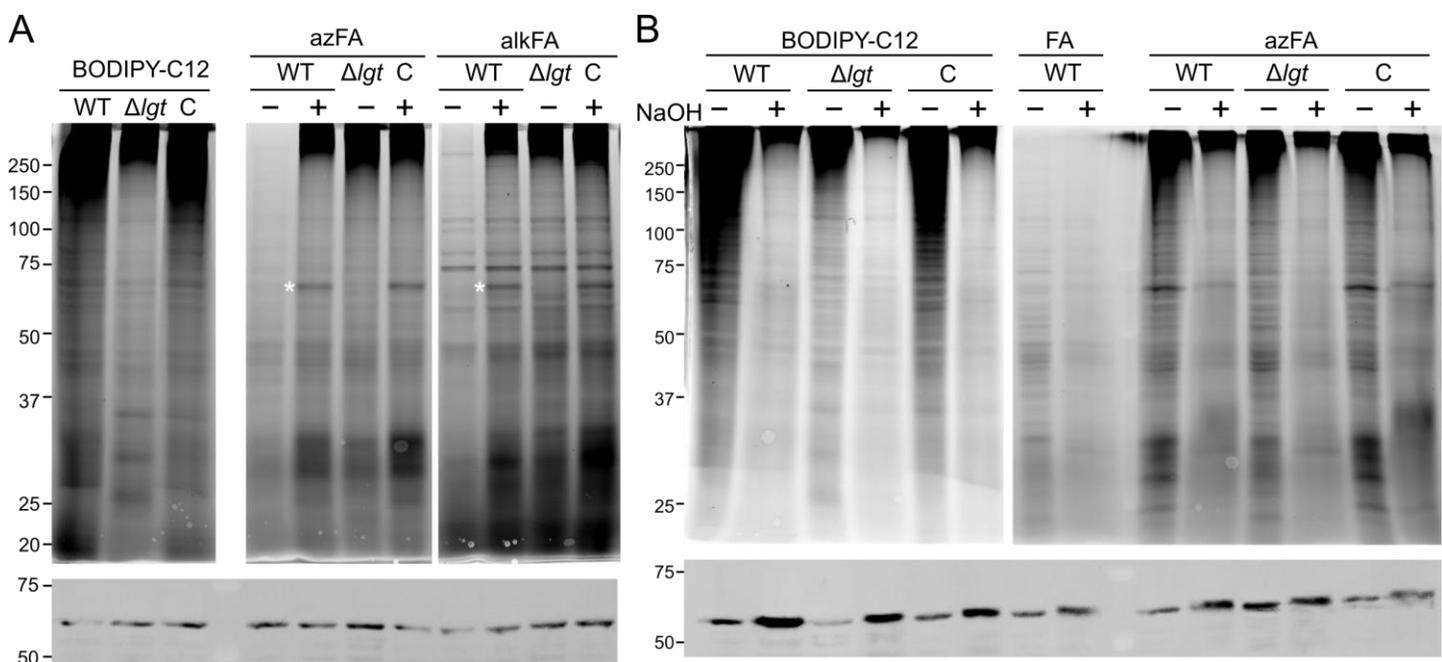
Figure 3. Metabolically incorporated fatty acid analogues depend on Lgt for incorporation and are labile to base hydrolysis. (A) *Msm* wild-type (WT), Δ*lgt*, or complement (C; Δ*lgt::lgt*) strainswere incubated with 5 µM BC12 or 20 µM azFA or alkFA for 1 h before harvesting. Total lysates of azFA- and alkFA-treated cells were subjected to CuAAC with alk-AZ488 or az-110, respectively. Wild type incubated with palmitic acid served as a negative control (−) for non-specific CuAAC-dependent signal. All samples in each panel were run on the same gel; lanes scanned in separate detection channels appear slightly separated. Data are representative of at least n = 3 independent experiments. GroEL immunoblot was used as a loading control. Data shown are representative of n = 3 independent experiments.

Having confirmed the incorporation of fatty acids into proteins, we next characterized the nature of the modification. We first sought to determine the contribution of lipoprotein biosynthesis. Since the lipoprotein processing enzymes Lgt, LspA, and Lnt are all essential, we used tetracycline-inducible CRISPRi[40] to knock down expression of the first enzyme, Lgt. We confirmed that *Mtb* survival on agar was compromised when a guide RNA targeting *lgt* (*rv1614*) was induced with anhydrotetracycline (ATc) (**Figure S3A**). However, prolonged ATc-induced depletion in liquid culture only moderately compromised survival or reduced RNA levels (**Figure S3B-D**). Metabolic labeling of proteins by BC12 was not noticeably affected by ATc even under conditions that produced the most pronounced growth defect (**Figure S3E**). These results are consistent with a CRISPRi screen showing that *lgt* is a relatively insensitive target, but therefore did not provide conclusive evidence regarding the involvement of Lgt in incorporating BC12 into proteins.

Unlike *Mtb*, *Msm* encodes two *lgt* homologues, *MSMEG_3222* and *MSMEG_5408*, with *MSMEG_3222* having higher homology to *Mtb lgt*. A previous study showed that Δ*MSMEG_3222* exhibited reduced incorporation of ^{14}C-palmitic acid into proteins compared to the wild type as well as altered localization of known lipoproteins, supporting its role in lipoprotein biosynthesis[15]. We constructed *Msm* Δ*MSMEG_3222* (**Figure S4**) and showed that incorporation of either BC12 or azFA was reduced by the loss of *MSMEG_3222* and this could be complemented (**Figure 3A**).

Lipoprotein modification generates ester and amide linkages are labile to base hydrolysis, as has been shown for protein O-mycoloylation in *Corynebacterium glutamicum*[34]. Sodium hydroxide treatment of BC12- and azFA-labeled total lysates reduced labeling, supporting the esterification/amidation of proteins by these fatty acid analogues (**Figure 3B**). Together, these

experiments show that metabolic incorporation of fatty acid analogues into proteins requires lipoprotein biosynthesis. While our data are consistent with tagged proteins being canonical lipoproteins, the possibility that lipid-modified proteins in *Msm* could also be O-mycoloylated is yet to be explored. Protein O-mycoloylation is mediated by the acyltransferase Cmt1 (also known as CMytC) in *Corynebacterium glutamicum*[41,42], but neither a corresponding enzyme nor confirmation of O-mycolylation itself has been reported in mycobacteria.

Lipoproteins are associated with the mycobacterial cell surface.

We previously identified proteins that interact with the lipoprotein LprG using crosslinking to a site-specifically incorporated photocrosslinking amino acid[43]. Among these was the outer membrane porin MspA, suggesting that despite lacking the Lol lipoprotein transport pathway, mycobacteria transport lipoproteins like LprG across the cell wall to the mycomembrane and/or cell surface. To test this hypothesis, we used several approaches to determine whether lipid-modified proteins are associated with the mycobacterial cell surface.

First, we hypothesized that the negative charges of the two sulfonic acid groups on the azido-fluorophore AZDye 488 would retard alk-AZ488 permeation into whole cells, since to the best of our knowledge, the outer leaflet of the mycomembrane is characterized by lipids that are either neutral (*e.g.*, acylated trehaloses) or negatively charged (*e.g.*, acylated sulfotrehaloses), suggesting an overall net negative charge that is also supported by measurements of *Msm* zeta potential[44,45]. Thus, we predicted that performing CuAAC with alk-AZ488 on whole cells labeled with azFA would selectively label lipid-modified proteins at the cell surface. This indeed yielded azFA-dependent protein labeling with a pattern distinct from that of similarly treated total lysates (**Figure 4A**).

Further, in contrast to lysates treated with DBCO (**Figure S2B, C**), whole cells subjected to SPAAC by incubation with DBCO-AZ488 showed azFA- and time-dependent labeling (0-30 min; **Figure 4B**). Importantly, longer incubation times (2 and 20 h) yielded labeling reminiscent of lysates treated with DBCO (**Figure 4C**, **Figure S2B-C**) and this labeling was not fully azFA-dependent.

These results support surface-specific tagging by SPAAC at shorter incubation times, with eventual

penetration of DBCO-AZ488 to yield azide-independent labeling of cytosolic proteins.
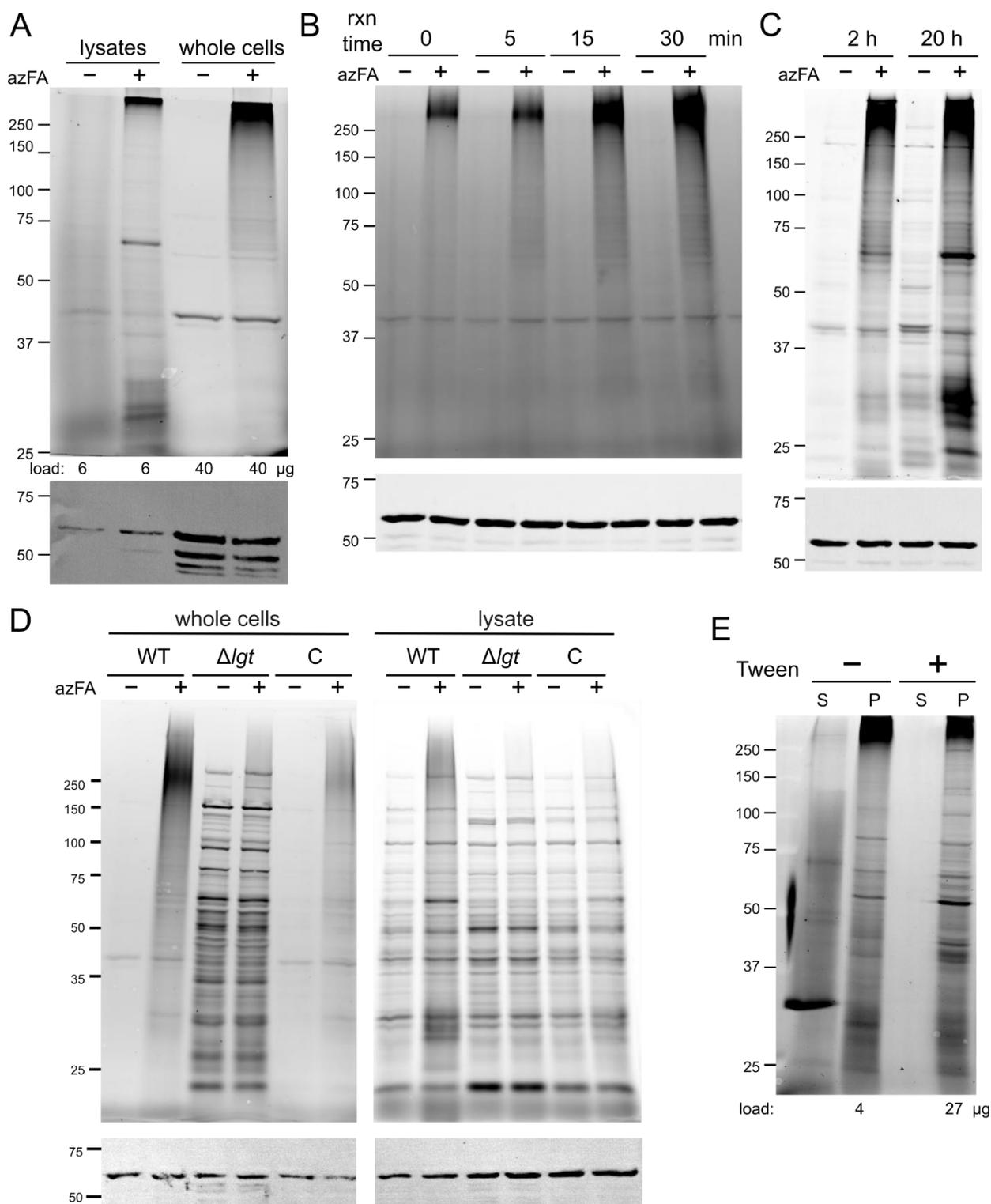
Figure 4. Click coupling and detergent extraction reveals lipid-modified proteins associated with the cell surface. A) *Msm* was incubated with 20 µM azFA for 2 h. CuAAC to alk-AZ488 was then performed on whole cells and total lysates. Protein load for lysate and whole-cell samples were normalized approximately for the degree of observed labeling. B), C) Same as in A) except azFA was incubated with *Msm* for the specified times with azFA prior to CuAAC to alk-AZ488 on whole cells. D)

Same as in A) using *Msm* wild-type, *ΔMSMEG_3222* (Δ*lgt*), and complement (C; Δ*lgt::lgt*) strains. E) *Msm* was cultured −/+ 0.5% Tween 80 and then incubated with azFA. Cells were extracted with 1% Tween 80 prior to lysis. Both the supernatant extract (S) and the total lysate of the remaining cell pellet (P) subjected to CuAAC and analyzed. Protein load for −/+ Tween pellet fractions were normalized approximately for the degree of observed labeling. GroEL immunoblot served as a loading control where relevant. Data are representative of n = 3 independent experiments.

We further reasoned that the lipoprotein-deficient strain Δ*MSMEG_3222* would have reduced levels of lipid-modified proteins also at the cell surface and tested this hypothesis by incubating wild-type, Δ*MSMEG_3222* and complement strains with AzFA follow by treatment of whole cells with DBCO-AZ488 (**Figure 4D**). Wild-type and complement strains indeed displayed similar patterns of AzFA-dependent labeling. However, rather than showing reduced labeling, Δ*MSMEG_3222* yielded AzFA-independent labeling similar to azide-independent labeling of lysates by DBCO reagents (**Figure 4C**, **Figure S2B-C**). This suggests that DBCO-AZ488 accumulates more quickly in Δ*MSMEG_3222* than the wild type and thus, that loss of *MSMEG_3222* compromises the cell envelope.

As an independent approach to detecting surface-associated proteins, we noted that mycobacteria are commonly cultured in the presence of Tween 80 detergent to disperse cells, but in the absence of detergent, they retain more surface-associated components such as carbohydrates and proteins, which can be subsequently extracted with Tween 80 for analysis[46]. We cultured cells in medium with and without detergent, incubated with azFA to label lipoproteins, and washed cells with detergent buffer to extract surface metabolites. Subsequent CuAAC to alk-AZ488 in detergent extracts and total lysates revealed labeled proteins that were extracted only from cells that had been cultured without detergent (**Figure 4E**).

Overall, these multiple lines of evidence support the conclusion that mycobacteria display lipid-modified proteins at the cell surface. This key finding implies that corresponding transport machinery is present in the cell wall and also has implications for the potential functions of mycobacterial lipoproteins, which have been assumed to reside in the outer leaflet of the inner membrane. Instead, our results show that lipid-anchored proteins are positioned at the interface with the host, perhaps

more consistent with proposed roles for lipoproteins in modulating the host response or otherwise serving as ligands for host receptors. With respect to lipoprotein transport machinery, while the Lol pathway has no homologues in mycobacteria, the soluble protein LolA and the lipoprotein LolB have low sequence identity but strong structural homology to the so-called lipid-binding lipoprotein family in mycobacteria (LprG, LppX, LprA, LprF)[22]. While all four proteins have been implicated in lipid binding and/or transport, LprG alone is conserved across mycobacteria and binds to a variety of triacyl lipids[47,48], consistent with a possible role in lipoprotein transport. Finally, the presence of both diacyl and triacyl lipoproteins in mycobacteria[15,19] suggests the tantalizing hypothesis that triacylation serves as a signal for lipoprotein transport across the cell wall. This would contrast with gram-negative lipoprotein transport in *E. coli*, in which recognition by the transport machinery is encoded by conserved N-terminal residues[49].

A photocrosslinking fatty acid enables the detection of lipid-protein interactions

Our above results contradict the commonly held assumption that mycobacteria do not transport lipoproteins beyond the inner membrane because they do not contain homologues of the Gram-negative Lol lipoprotein transport pathway. In the Lol pathway, LolA solubilizes and shuttles lipoprotein cargo across the cell wall by binding to the lipid modification within the aqueous periplasm[50]. Based on this model, we posited that metabolic labeling would also afford an opportunity to detect lipid-protein interactions, towards identifying components of the transport machinery and other interacting proteins. *Msm* was incubated with a palmitic acid analogue containing a terminal alkyne and a photoactivatable diazirine crosslinker (photoclick-FA)[51] and UV-irradiated prior to lysis and CuAAC to a fluorescent azide (az-AZ488). In the absence of UV irradiation, feeding with photoclick-FA revealed a similar protein labeling pattern (**Figure 5**) to that of other fatty acid analogues (**Figure 2, 4**). However, only treatment with photoclick-FA yielded additional protein bands at higher molecular weights, consistent with the formation of lipoprotein-protein adducts due to crosslinking of the lipid modification to an interacting protein (**Figure 5**).

We found that feeding with a photoclick fatty acid yielded UV irradiation-dependent adducts. We note that based on our analysis of BC12-containing lipids, photoclick-FA is likely also incorporated into lipids that, if proximal to or bound by proteins, would form protein-lipid adducts that also contribute to the observed UV-dependent signal. This approach offers an additional opportunity identify lipid-interacting proteins, as has been done with analogous trehalose monomycolate lipid analogues, although additional work will be necessary to deconvolute proteins that interact with lipids vs. protein lipid modifications.
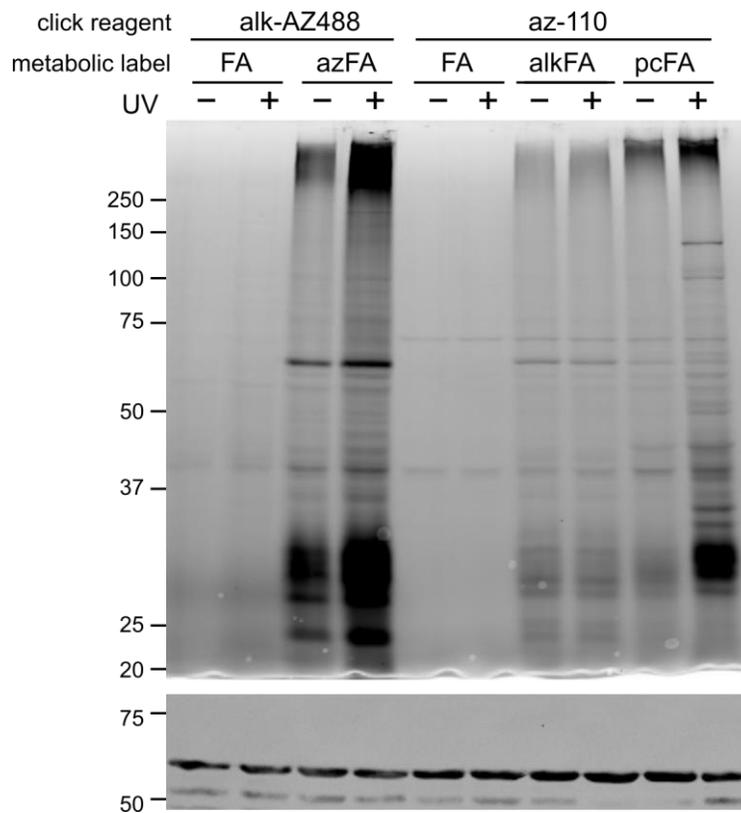
Figure 5. Incorporation of a photoclick-FA in *Msm* yields UV-dependent adducts. *Msm* was incubated with palmitic acid (FA), azFA, alkFA, or pcFA for 30 min. and then UV irradiated for a total of 30 min. Total lysates were subjected to CuAC with either alk-AZ488 or az-110 as indicated. GroEL immunoblot served as a loading control. Data are representative of n = 3 independent experiments.

Overall, our results expanding and validating metabolic labeling of protein lipid modifications pave the way for the broader use of this method to track the biosynthesis, inhibition, and binding of lipoproteins not only in mycobacteria, but also in other bacteria in which these processes are relatively poorly understood.

METHODS

Bacterial strains and growth. All strains, oligonucleotides and plasmids used in this study are detailed in Tables S1-S3. *Mycobacterium smegmatis* mc[2]155 (*Msm*; ATCC 700084) was cultured in Middlebrook 7H9 medium (HI MEDIA) with 1% w/v casamino acids (VWR), 0.2% w/v glucose, 0.05% v/v Tween 80 at 37 °C with shaking at 250 rpm unless otherwise noted. For growth on solid medium, *Msm* was propagated on Middlebrook 7H11 agar with 10% v/v albumin-dextrose-catalase (ADC) supplement (BD), 0.5% v/v glycerol, 0.05% v/v Tween 80. *Msm* Δ*mceG* and Δ*mceG*::*mceG* strains[35] (gift of Damien Ekiert and Gira Bhabha) were selected with 50 µg/mL hygromycin (Δ*mceG*) or 25 µg/mL hygromycin and 10 µg/mL zeocin (Δ*mceG::mceG*). Bacteria were selected on kanamycin (25 µg/mL) or hygromycin (50 µg/mL) as appropriate (Table S3). Cells were harvested by centrifugation at 4,000 x g for 5 min and all steps were performed at 22 °C unless otherwise indicated.

Generation and confirmation of *Msm* Δ*MSMEG_3222*. A targeted knockout strain of *MSMEG_3222* was generated in *Msm* as previously reported[52]. Briefly, 5' (321 bp) and 3' (248 bp) sequences flanking *MSMEG_3222* were cloned on either side of a hygromycin resistance cassette via the HindIII and XbaI sites of pJSC407 using In-Fusion Cloning (Takara Bio). The resulting plasmid was sequence confirmed and used as a template for PCR using oligonucleotides omlp1085 and omlp1088 (Table S2) to generate a recombineering substrate that was transformed directly into *Msm::*pNIT-RecET expressing the recombinase following treatment with isovaleronitrile. Successful recombinants were selected on agar containing hygromycin and individual clones confirmed by PCR (Figure S1) and sequencing. A complement plasmid was generated by cloning *MSMEG_3222* (including 998 nt 5' of the start codon as a native promoter) into the integrating plasmid pMV306 via the XbaI and ClaI sites using In-Fusion Cloning. The resulting plasmid was sequence confirmed, transformed into Δ*MSMEG_3222* and selected on agar containing kanamycin.

Metabolic incorporation of fatty acids in *Msm*. *Msm* was cultured to mid-logarithmic phase (OD$_{600}$ ~1.5) and then diluted to OD$_{600}$ 0.5 and incubated for 2 h (unless otherwise specified) at 37 °C with palmitate (FA; Acros Organics), BODIPY-C12 (BC12; ThermoFisher), azido palmitic acid (azFA;

Click Chemistry Tools/Vector Laboratories), alkynyl palmitic acid (alkFA; Vector Laboratories), Click Tag™ palmitic acid (photoclick-FA; Cayman Chemical), or 12:0 N-biotinyl fatty acid (biotin-FA; Avanti Lipids) at the final concentrations indicated in each figure (0-20 µM). All fatty acids were dissolved in DMSO and diluted such that the final DMSO concentration was 0.6% for 12:0 N-biotinyl fatty acid and 0.05-0.1% for all others. Experiments involving total lysates resulting from BC12 or azFA treatment were derived from 10 mL of bacterial culture per condition. Experiments in which whole cells were subjected to copper-mediated or strain-promoted azide-alkyne cycloaddition (CuAAC or SPAAC) used 15 mL of bacterial culture per condition. Experiments with photoclick-FA used 30-40 mL of bacterial culture per condition. After incubation with fatty acid, cultures were harvested and washed three times with an equal volume of PBS with 0.05% v/v Tween 80 (PBST). Pellets were processed immediately or stored at -80 °C until further use.

Lipid extraction and analysis. Lipids were extracted as reported. Briefly, following metabolic incorporation of BC12 into *Msm* as described above, cells were washed and cultured for a further 2 h before harvesting by centrifugation. The pellet was resuspended in water and subjected to modified Bligh and Dyer extraction as follows: 1:2 chloroform:methanol (C:M) was added to a final ratio of 1:2:0.8 C:M:water (C:M:W) before storage at -20 °C until further processing. After samples were allowed to warm to 22 °C, chloroform and water were added with vortexing to obtain 1:1:0.8 C:M:W followed by centrifugation at 10,000 x g for 5 min. The lower phase was transferred to a fresh tube and allowed to dried overnight. The resulting film was resuspended in 2:1 C:M in 1/16th the original extraction volume. A migration standard for TAG containing BC12 was generated from BC12-treated THP-1 cells as described.

Briefly, 3 x 10^6 THP-1 monocytes were differentiated into macrophages using 100 µM PMA at a density of 0.6 million cells/ml for 24 h, followed by 2 days in media without PMA. Subsequently, BC12 was added to 1 µM and cells were cultured for an additional 24 h. Medium was removed and the monolayer was washed twice with PBS. Cells were then lysed in 0.5 mL PBS with 1% (v/v) TritonX-100. Four volumes of methanol:chloroform (2:1) was added to the lysate and vortexed for 30

seconds. This was followed by addition of one volume each of 50 mM citric acid, water, and chloroform with vortexing. After centrifugation at 10,000 g for 10 min, the lower phase was isolated, dried and resuspended in 200 μL chloroform: methanol (2:1). Five μL of each sample was resolved on aluminum-backed TLC silica gel 60 plates (Supelco) in 100:14:0.8 C:M:W or 70:30:1 hexanes:diethyl ether:acetone. TLCs were scanned for BODIPY fluorescence with a Sapphire Bioimager (Azure Biosystems).

Detergent extraction of whole cells. *Msm* was cultured to mid-logarithmic phase (OD$_{600}$ ~1.5) and then subcultured to OD$_{600}$ ~0.02 in 10 mL culture medium with or without 0.05% Tween 80 and grown overnight to a final OD$_{600}$ ~1.5, as determined from the dispersed culture containing Tween 80. Both cultures were diluted to OD$_{600}$ 0.5 and incubated with 5 μM BC12 for 2 h at 37 °C. Harvested cells were washed twice with an equal volume of PBS. The final cell pellet was resuspended in 800 μL PBS with 1% v/v Tween 80. The suspension was transferred to a 1.5-mL microfuge tube and incubated for 30 min with gentle mixing at 22 °C on an orbital shaker. Cells were harvested by centrifugation at 10,000 x*g* for 10 min and 500 μL supernatant was collected as the detergent extract. The remaining cell pellet was processed for total lysate.

UV irradiation for photo-crosslinking. After incubation with photoclick-FA, cells (corresponding to 30-40 mL culture; see section "Metabolic labeling with fatty acids") were harvested and resuspended in 2 mL PBST. One 1-mL aliquot was pipetted into a 6-well multiwell plate; the other was kept on ice as the no-irradiation (-UV) control. The multiwell plate was placed on ice and irradiated from above with a UV transilluminator for a total of 30 min with gentle manual agitation every 5 min.

Preparation of total lysates. Each cell pellet was resuspended in 800-100 μL PBS and added to a 2-mL microfuge tube containing ~0.5 mL 0.1-mm zirconia beads. Cells were lysed at 6 m/s for 30 s (Bead Ruptor 12, Omni International) for a total of 4 cycles with samples placed on ice for 5 min between cycles. Lysates were clarified by centrifugation at 10,000 x*g* at 4 °C for 10 min and the clarified supernatants were transferred to fresh tubes.

Azide-alkyne coupling. The protein concentrations of total lysates were determined by the BCA assay (Pierce) and normalized to 0.65-1 mg/mL depending on the concentration of the most dilute sample in a given experiment. Copper-mediated azide-alkyne cycloaddition (CuAAC) was performed as previously described[5] with 100 µL normalized total lysate and a final concentration of 25 µM AZDye 488 Alkyne (alk-AZ488; Vector Laboratories), azido-PEG3-carboxyrhodamine 110 (az-110; ThermoFisher), or AZDye 488 Azide (az-AZ488; Vector Laboratories) and incubated at 22 °C with orbital shaking. The reaction time was 1 h for Figure 1C and 5 min for all other experiments. The reaction was quenched with 1 mM EDTA and 1X Laemmli sample loading buffer final concentration.

For strain-promoted reactions (SPAAC) with total lysates, 100 µL normalized lysate was incubated with 25 µM AZDye 488 DBCO (DBCO-AZ488) or Biotin-PEG4-DBCO (DBCO-biotin; Vector Laboratories) incubated for 1 h at 22 °C with orbital shaking. For SPAAC with whole cells, the cell pellet from 12.5 mL of culture (OD_{600} ~0.8) was resuspended in 800 µL PBS and incubated with 25 µM DBCO-AZ488 at 22 °C for 0-20 h. Cells were harvested and washed 4 times with an equal volume of PBST before storage or processing for total lysates.

Alkaline treatment of total lysates. Lysates were thawed on ice and normalized to 1 mg/mL with PBS in a total volume of 60 µL and sodium hydroxide added to a final concentration of 0.1 M. Lysates were incubated at 37 °C at 250 rpm for 30 min and then neutralized with 0.1 M acetic acid before adding Laemmli sample loading buffer to 1X final concentration.

Protein analysis by SDS-PAGE. Protein concentrations of clarified lysates (see "Preparation of total lysates" above) were determined by BCA assay (Pierce) and normalized to 0.75 mg/mL with PBS and Laemmli sample loading buffer added to 1X final concentration. To reduce observed smearing of the fluorescence signal, samples were not boiled before SDS-PAGE. The gel was scanned for fluorescence (Sapphire Bioimager, Azure Biosystems). For GroEL immunoblotting, proteins were transferred to nitrocellulose membranes (Trans-Blot Semi-Dry Transfer Cell; Bio-Rad) and probed with α-GroEL (1:5000, sc-58170, Santa Cruz Biotechnology) and goat anti-mouse IR Dye 800CW (1:15,000, 926−32210, LI-COR) or with streptavidin IR-Dye 680LT (1:1000, 926-68031, LI-

COR). Images were analyzed in ImageJ and normalized lane fluorescence was calculated by integrating well-resolved signal within a single lane (from ~25-100 kDa) and dividing by the integrated GroEL signal.

ACKNOWLEDGMENTS

FUNDING SOURCES

REFERENCES

(1)   Jarlier, V.; Nikaido, H. Permeability Barrier to Hydrophilic Solutes in Mycobacterium Chelonei. *Journal of Bacteriology* **1990**, *172* (3), 1418–1423. https://doi.org/10.1128/jb.172.3.1418-1423.1990.

(2)   Jarlier, V.; Gutmann, L.; Nikaido, H. Interplay of Cell Wall Barrier and Beta-Lactamase Activity Determines High Resistance to Beta-Lactam Antibiotics in Mycobacterium Chelonae. *Antimicrobial Agents and Chemotherapy* **1991**, *35* (9), 1937–1939. https://doi.org/10.1128/AAC.35.9.1937.

(3)   Jaisinghani, N.; Previti, M. L.; Andrade, J.; Askenazi, M.; Ueberheide, B.; Seeliger, J. C. Proteomics from Compartment-Specific APEX2 Labeling in Mycobacterium Tuberculosis Reveals Type VII Secretion Substrates in the Cell Wall. *Cell Chemical Biology* **2024**, *31* (3), 523-533.e4. https://doi.org/10.1016/j.chembiol.2023.10.013.

(4)   Perkowski, E. F.; Zulauf, K. E.; Weerakoon, D.; Hayden, J. D.; Ioerger, T. R.; Oreper, D.; Gomez, S. M.; Sacchettini, J. C.; Braunstein, M. The EXIT Strategy: An Approach for Identifying Bacterial

Proteins Exported during Host Infection. *mBio* **2017**, *8* (2), e00333-17. https://doi.org/10.1128/mBio.00333-17.

(5) Kavunja, H. W.; Biegas, K. J.; Banahene, N.; Stewart, J. A.; Piligian, B. F.; Groenevelt, J. M.; Sein, C. E.; Morita, Y. S.; Niederweis, M.; Siegrist, M. S.; Swarts, B. M. Photoactivatable Glycolipid Probes for Identifying Mycolate–Protein Interactions in Live Mycobacteria. *J. Am. Chem. Soc.* **2020**. https://doi.org/10.1021/jacs.0c01065.

(6) Sassetti, C. M.; Boyd, D. H.; Rubin, E. J. Genes Required for Mycobacterial Growth Defined by High Density Mutagenesis. *Molecular Microbiology* **2003**, *48* (1), 77–84. https://doi.org/10.1046/j.1365-2958.2003.03425.x.

(7) Griffin, J. E.; Gawronski, J. D.; DeJesus, M. A.; Ioerger, T. R.; Akerley, B. J.; Sassetti, C. M. High-Resolution Phenotypic Profiling Defines Genes Essential for Mycobacterial Growth and Cholesterol Catabolism. *PLOS Pathogens* **2011**, *7* (9), e1002251. https://doi.org/10.1371/journal.ppat.1002251.

(8) DeJesus, M. A.; Gerrick, E. R.; Xu, W.; Park, S. W.; Long, J. E.; Boutte, C. C.; Rubin, E. J.; Schnappinger, D.; Ehrt, S.; Fortune, S. M.; Sassetti, C. M.; Ioerger, T. R. Comprehensive Essentiality Analysis of the Mycobacterium Tuberculosis Genome via Saturating Transposon Mutagenesis. *mBio* **2017**, *8* (1). https://doi.org/10.1128/mBio.02133-16.

(9) Bosch, B.; DeJesus, M. A.; Poulton, N. C.; Zhang, W.; Engelhart, C. A.; Zaveri, A.; Lavalette, S.; Ruecker, N.; Trujillo, C.; Wallach, J. B.; Li, S.; Ehrt, S.; Chait, B. T.; Schnappinger, D.; Rock, J. M. Genome-Wide Gene Expression Tuning Reveals Diverse Vulnerabilities of M. Tuberculosis. *Cell* **2021**, S0092867421008242. https://doi.org/10.1016/j.cell.2021.06.033.

(10) Rezwan, M.; Grau, T.; Tschumi, A.; Sander, P. Lipoprotein Synthesis in Mycobacteria. *Microbiology* **2007**, *153* (3), 652–658. https://doi.org/10.1099/mic.0.2006/000216-0.

(11) Sutcliffe, I. C.; Harrington, D. J. Lipoproteins of Mycobacterium Tuberculosis: An Abundant and Functionally Diverse Class of Cell Envelope Components. *FEMS Microbiology Reviews* **2004**, *28* (5), 645–659. https://doi.org/10.1016/j.femsre.2004.06.002.

(12) Bigi, M. M.; Forrellad, M. A.; García, J. S.; Blanco, F. C.; Vázquez, C. L.; Bigi, F. An Update on Mycobacterium Tuberculosis Lipoproteins. *Future Microbiology* **2023**. https://doi.org/10.2217/fmb-2023-0088.

(13) Nakayama, H.; Kurokawa, K.; Lee, B. L. Lipoproteins in Bacteria: Structures and Biosynthetic Pathways. *The FEBS Journal* **2012**, *279* (23), 4247–4268. https://doi.org/10.1111/febs.12041.

(14) McDonough, J. A.; McCann, J. R.; Tekippe, E. M.; Silverman, J. S.; Rigel, N. W.; Braunstein, M. Identification of Functional Tat Signal Sequences in Mycobacterium Tuberculosis Proteins. *J Bacteriol* **2008**, *190* (19), 6428–6438. https://doi.org/10.1128/JB.00749-08.

(15) Tschumi, A.; Grau, T.; Albrecht, D.; Rezwan, M.; Antelmann, H.; Sander, P. Functional Analyses of Mycobacterial Lipoprotein Diacylglyceryl Transferase and Comparative Secretome Analysis of a Mycobacterial Lgt Mutant. *Journal of Bacteriology* **2012**, *194* (15), 3938–3949. https://doi.org/10.1128/JB.00127-12.

(16) Sander, P.; Rezwan, M.; Walker, B.; Rampini, S. K.; Kroppenstedt, R. M.; Ehlers, S.; Keller, C.; Keeble, J. R.; Hagemeier, M.; Colston, M. J.; Springer, B.; Böttger, E. C. Lipoprotein Processing Is Required for Virulence of Mycobacterium Tuberculosis. *Molecular Microbiology* **2004**, *52* (6), 1543–1552. https://doi.org/10.1111/j.1365-2958.2004.04041.x.

(17) Tschumi, A.; Nai, C.; Auchli, Y.; Hunziker, P.; Gehrig, P.; Keller, P.; Grau, T.; Sander, P. Identification of Apolipoprotein N-Acyltransferase (Lnt) in Mycobacteria. *The Journal of biological chemistry* **2009**, *284* (40), 27146–27156. https://doi.org/10.1074/jbc.M109.022715.

(18) Banaei, N.; Kincaid, E. Z.; Lin, S.-Y. G.; Desmond, E.; Jacobs, W. R.; Ernst, J. D. Lipoprotein Processing Is Essential for Resistance of Mycobacterium Tuberculosis to Malachite Green. *Antimicrob Agents Chemother* **2009**, *53* (9), 3799–3802. https://doi.org/10.1128/AAC.00647-09.

(19) Brulle, J. K.; Tschumi, A.; Sander, P. Lipoproteins of Slow-Growing Mycobacteria Carry Three Fatty Acids and Are N-Acylated by Apolipoprotein N-Acyltransferase BCG_2070c. *BMC microbiology* **2013**, *13*, 223. https://doi.org/10.1186/1471-2180-13-223.

(20) Gurcha, S. S.; Baulard, A. R.; Kremer, L.; Locht, C.; Moody, D. B.; Muhlecker, W.; Costello, C. E.; Crick, D. C.; Brennan, P. J.; Besra, G. S. Ppm1, a Novel Polyprenol Monophosphomannose Synthase from Mycobacterium Tuberculosis. *Biochem J* **2002**, *365* (Pt 2), 441–450. https://doi.org/10.1042/BJ20020107.

(21) Grabowicz, M. Lipoprotein Transport: Greasing the Machines of Outer Membrane Biogenesis. *BioEssays* **2018**, *40* (4), 1700187. https://doi.org/10.1002/bies.201700187.

(22) Touchette, M. H.; Seeliger, J. C. Transport of Outer Membrane Lipids in Mycobacteria. *Biochimica et Biophysica Acta (BBA) - Molecular and Cell Biology of Lipids* **2017**, *1862* (11), 1340–1354. https://doi.org/10.1016/j.bbalip.2017.01.005.

(23) Mawuenyega, K. G.; Forst, C. V.; Dobos, K. M.; Belisle, J. T.; Chen, J.; Bradbury, E. M.; Bradbury, A. R.; Chen, X. Mycobacterium Tuberculosis Functional Network Analysis by Global Subcellular Protein Profiling. *Molecular biology of the cell* **2005**, *16* (1), 396–404. https://doi.org/10.1091/mbc.E04-04-0329.

(24) Wolfe, L. M.; Mahaffey, S. B.; Kruh, N. A.; Dobos, K. M. Proteomic Definition of the Cell Wall of Mycobacterium Tuberculosis. *J Proteome Res* **2010**, *9* (11), 5816–5826. https://doi.org/10.1021/pr1005873.

(25) Bell, C.; Smith, G. T.; Sweredoski, M. J.; Hess, S. Characterization of the Mycobacterium Tuberculosis Proteome by Liquid Chromatography Mass Spectrometry-Based Proteomics Techniques: A Comprehensive Resource for Tuberculosis Research. *Journal of proteome research* **2012**, *11* (1), 119–130. https://doi.org/10.1021/pr2007939.

(26) Feltcher, M. E.; Gunawardena, H. P.; Zulauf, K. E.; Malik, S.; Griffin, J. E.; Sassetti, C. M.; Chen, X.; Braunstein, M. Label-Free Quantitative Proteomics Reveals a Role for the Mycobacterium Tuberculosis SecA2 Pathway in Exporting Solute Binding Proteins and Mce Transporters to the Cell Wall. *Molecular & cellular proteomics : MCP* **2015**, *14* (6), 1501–1516. https://doi.org/10.1074/mcp.M114.044685.

(27) Parra, J.; Marcoux, J.; Poncin, I.; Canaan, S.; Herrmann, J. L.; Nigou, J.; Burlet-Schiltz, O.; Rivière, M. Scrutiny of Mycobacterium Tuberculosis 19 kDa Antigen Proteoforms Provides New Insights in the Lipoglycoprotein Biogenesis Paradigm. *Sci Rep* **2017**, *7* (1), 43682. https://doi.org/10.1038/srep43682.

(28) Young, D. B.; Garbe, T. R. Lipoprotein Antigens of Mycobacterium Tuberculosis. *Res Microbiol* **1991**, *142* (1), 55–65. https://doi.org/10.1016/0923-2508(91)90097-t.

(29) Sulzenbacher, G.; Canaan, S.; Bordat, Y.; Neyrolles, O.; Stadthagen, G.; Roig-Zamboni, V.; Rauzier, J.; Maurin, D.; Laval, F.; Daffé, M.; Cambillau, C.; Gicquel, B.; Bourne, Y.; Jackson, M. LppX Is a Lipoprotein Required for the Translocation of Phthiocerol Dimycocerosates to the Surface of Mycobacterium Tuberculosis. *EMBO J.* **2006**, *25* (7), 1436–1444. https://doi.org/10.1038/sj.emboj.7601048.

(30) Daniel, J.; Maamar, H.; Deb, C.; Sirakova, T. D.; Kolattukudy, P. E. Mycobacterium Tuberculosis Uses Host Triacylglycerol to Accumulate Lipid Droplets and Acquires a Dormancy-Like Phenotype in Lipid-Loaded Macrophages. *PLoS Pathog* **2011**, *7* (6), e1002093. https://doi.org/10.1371/journal.ppat.1002093.

(31) Nazarova, E. V.; Montague, C. R.; La, T.; Wilburn, K. M.; Sukumar, N.; Lee, W.; Caldwell, S.; Russell, D. G.; VanderVen, B. C. Rv3723/LucA Coordinates Fatty Acid and Cholesterol Uptake in Mycobacterium Tuberculosis. *eLife* **2017**, *6*, e26969. https://doi.org/10.7554/eLife.26969.

(32) Nazarova, E. V.; Podinovskaia, M.; Russell, D. G.; VanderVen, B. C. Flow Cytometric Quantification of Fatty Acid Uptake byMycobacterium Tuberculosis in Macrophages. *Bio Protoc* **2018**, *8* (4), e2734. https://doi.org/10.21769/BioProtoc.2734.

(33) Rangan, K. J.; Yang, Y.-Y.; Charron, G.; Hang, H. C. Rapid Visualization and Large-Scale Profiling of Bacterial Lipoproteins with Chemical Reporters. *J. Am. Chem. Soc.* **2010**, *132* (31), 10628–10629. https://doi.org/10.1021/ja101387b.

(34) Issa, H.; Huc-Claustre, E.; Reddad, T.; Bonade Bottino, N.; Tropis, M.; Houssin, C.; Daffe, M.; Bayan, N.; Dautin, N. Click-Chemistry Approach to Study Mycoloylated Proteins: Evidence for

PorB and PorC Porins Mycoloylation in Corynebacterium Glutamicum. *PloS one* **2017**, *12* (2), e0171955. https://doi.org/10.1371/journal.pone.0171955.

(35) Chen, J.; Fruhauf, A.; Fan, C.; Ponce, J.; Ueberheide, B.; Bhabha, G.; Ekiert, D. C. Structure of an Endogenous Mycobacterial MCE Lipid Transporter. *Nature* **2023**, *620* (7973), 445–452. https://doi.org/10.1038/s41586-023-06366-0.

(36) Joshi, S. M.; Pandey, A. K.; Capite, N.; Fortune, S. M.; Rubin, E. J.; Sassetti, C. M. Characterization of Mycobacterial Virulence Genes through Genetic Interaction Mapping. *Proc Natl Acad Sci U S A* **2006**, *103* (31), 11760–11765. https://doi.org/10.1073/pnas.0603179103.

(37) Chen, Y.; Wang, Y.; Chng, S.-S. A Conserved Membrane Protein Negatively Regulates Mce1 Complexes in Mycobacteria. *Nat Commun* **2023**, *14*, 5897. https://doi.org/10.1038/s41467-023-41578-y.

(38) García-Fernández, J.; Papavinasasundaram, K.; Galán, B.; Sassetti, C. M.; García, J. L. Unravelling the Pleiotropic Role of the MceG ATPase in Mycobacterium Smegmatis. *Environ Microbiol* **2017**, *19* (7), 2564–2576. https://doi.org/10.1111/1462-2920.13771.

(39) van Geel, R.; Pruijn, G. J. M.; van Delft, F. L.; Boelens, W. C. Preventing Thiol-Yne Addition Improves the Specificity of Strain-Promoted Azide–Alkyne Cycloaddition. *Bioconjugate Chem.* **2012**, *23* (3), 392–398. https://doi.org/10.1021/bc200365k.

(40) Wong, A. I.; Rock, J. M. CRISPR Interference (CRISPRi) for Targeted Gene Silencing in Mycobacteria. *Methods Mol Biol* **2021**, *2314*, 343–364. https://doi.org/10.1007/978-1-0716-1460-0_16.

(41) De Sousa-D'Auria, C.; Kacem, R.; Puech, V.; Tropis, M.; Leblon, G.; Houssin, C.; Daffé, M. New Insights into the Biogenesis of the Cell Envelope of Corynebacteria: Identification and Functional Characterization of Five New Mycoloyltransferase Genes in Corynebacterium Glutamicum. *FEMS Microbiology Letters* **2003**, *224* (1), 35–44. https://doi.org/10.1016/S0378-1097(03)00396-3.

(42) Huc, E.; de Sousa-D'Auria, C.; de la Sierra-Gallay, I. L.; Salmeron, C.; van Tilbeurgh, H.; Bayan, N.; Houssin, C.; Daffé, M.; Tropis, M. Identification of a Mycoloyl Transferase Selectively Involved in O-Acylation of Polypeptides in Corynebacteriales. *J Bacteriol* **2013**, *195* (18), 4121–4128. https://doi.org/10.1128/JB.00285-13.

(43) Touchette, M. H.; Van Vlack, E. R.; Bai, L.; Kim, J.; Cognetta, A. B.; Previti, M. L.; Backus, K. M.; Martin, D. W.; Cravatt, B. F.; Seeliger, J. C. A Screen for Protein–Protein Interactions in Live Mycobacteria Reveals a Functional Link between the Virulence-Associated Lipid Transporter LprG and the Mycolyltransferase Antigen 85A. *ACS Infect. Dis.* **2017**, *3* (5), 336–348. https://doi.org/10.1021/acsinfecdis.6b00179.

(44) Ayala-Torres, C.; Hernández, N.; Galeano, A.; Novoa-Aponte, L.; Soto, C.-Y. Zeta Potential as a Measure of the Surface Charge of Mycobacterial Cells. *Ann Microbiol* **2014**, *64* (3), 1189–1195. https://doi.org/10.1007/s13213-013-0758-y.

(45) Smith, D. E.; Dhinojwala, A.; Moore, F. B.-G. Effect of Substrate and Bacterial Zeta Potential on Adhesion of Mycobacterium Smegmatis. *Langmuir* **2019**, *35* (21), 7035–7042. https://doi.org/10.1021/acs.langmuir.8b03920.

(46) Sani, M.; Houben, E. N. G.; Geurtsen, J.; Pierson, J.; de Punder, K.; van Zon, M.; Wever, B.; Piersma, S. R.; Jiménez, C. R.; Daffé, M.; Appelmelk, B. J.; Bitter, W.; van der Wel, N.; Peters, P. J. Direct Visualization by Cryo-EM of the Mycobacterial Capsular Layer: A Labile Structure Containing ESX-1-Secreted Proteins. *PLoS Pathog* **2010**, *6* (3), e1000794. https://doi.org/10.1371/journal.ppat.1000794.

(47) Drage, M. G.; Tsai, H.-C.; Pecora, N. D.; Cheng, T.-Y.; Arida, A. R.; Shukla, S.; Rojas, R. E.; Seshadri, C.; Moody, D. B.; Boom, W. H.; Sacchettini, J. C.; Harding, C. V. Mycobacterium Tuberculosis Lipoprotein LprG (Rv1411c) Binds Triacylated Glycolipid Agonists of Toll-like Receptor 2. *Nat. Struct. Mol. Biol.* **2010**, *17* (9), 1088–1095. https://doi.org/10.1038/nsmb.1869.

(48) Shukla, S.; Richardson, E. T.; Athman, J. J.; Shi, L.; Wearsch, P. A.; McDonald, D.; Banaei, N.; Boom, W. H.; Jackson, M.; Harding, C. V. Mycobacterium Tuberculosis Lipoprotein LprG Binds

Lipoarabinomannan and Determines Its Cell Envelope Localization to Control Phagolysosomal Fusion. *PLOS Pathogens* **2014**, *10* (10), e1004471. https://doi.org/10.1371/journal.ppat.1004471.

(49) Masuda, K.; Matsuyama, S.; Tokuda, H. Elucidation of the Function of Lipoprotein-Sorting Signals That Determine Membrane Localization. *Proceedings of the National Academy of Sciences* **2002**, *99* (11), 7390–7395. https://doi.org/10.1073/pnas.112085599.

(50) Okuda, S.; Tokuda, H. Lipoprotein Sorting in Bacteria. *Annual Review of Microbiology* **2011**, *65* (1), 239–259. https://doi.org/10.1146/annurev-micro-090110-102859.

(51) Peng, T.; Hang, H. C. Bifunctional Fatty Acid Chemical Reporter for Analyzing S-Palmitoylated Membrane Protein–Protein Interactions in Mammalian Cells. *J. Am. Chem. Soc.* **2015**, *137* (2), 556–559. https://doi.org/10.1021/ja502109n.

(52) Murphy, K. C.; Papavinasasundaram, K.; Sassetti, C. M. Mycobacterial Recombineering. *Methods in molecular biology* **2015**, *1285*, 177–199. https://doi.org/10.1007/978-1-4939-2450-9_10.